An Electrochemical Evaluation of Synthesized Coumarin-Azo Dyes as Potential Corrosion Inhibitors for Mild Steel in 1 M HCl Medium

Mohd Hamizi Yusoff [1], Mohamad Nurul Azmi[1,2,*], Mohd Hazwan Hussin[1,*], Hasnah Osman[1], Pandian Bothi Raja[1], Afidah Abdul Rahim[1], Khalijah Awang[3]

[1] School of Chemical Sciences, Universiti Sains Malaysia, 11800 Minden, Pulau Pinang, Malaysia
[2] Malaysian Institute of Pharmaceuticals & Nutraceuticals, NIBM, Ministry of Science, Technology and Innovation (MOSTI), Pulau Pinang, 11700 Malaysia
[3] Department of Chemistry, Faculty of Science, University of Malaya, 50603 Kuala Lumpur
*E-mail: mnazmi@usm.my; mhh@usm.my

The anti corrosion properties of mild steel were studied in 1.0 M HCl medium with azo-coumarin dyes inhibitor by electrochemical impedance and potentiodynamic polarization measurements. The azo-coumarin dyes 8-10 were synthesized by coupling reaction between diazonium salt of aniline derivatives with 4-hydroxycoumarin under basic condition. The result showed that inhibition efficiency was found to increase (shown average *IE* > 80%), with increasing the concentration of azo-coumarin dyes, and their adsorption over mild steel surface found to obey Langmuir adsorption isotherm. Furthermore, the Langmuir adsorption isotherm parameters made evident that corrosion inhibition proceeds through physisorption mode of interaction. After corrosion evaluation, mild steel's surface morphology was screened via SEM - EDX analysis which showed an improved surface in the presence of azo-coumarin dye derivatives.

1. INTRODUCTION

Mild steel (MS) is one of the extensively used construction / fabrication materials over boilers, cooling towers and oil / gas pipelines, which is usually operated at high temperature and pressure with aggressive chemicals [1]. In particular, hydrochloric acid is regularly used in industries for descaling purposes, which is corrosive and difficult to control corrosion over construction metals / materials. Hence, an immense care is mandatorily required during handling and their applications over the metals surfaces even at dilute concentrations. Usually, iron and their alloys degraded easily during descaling

process with mineral acids like hydrochloric acid, which ended in loss of metal resources and economy.

Reducing the metal corrosion rate over industries not only saves the metal resources / industrial economy, but also enhance the lifespan of the equipment, which subsequently reducing the disbanding of toxic metals / materials from the components into the surrounding environment [2]. Hence, over industrial sectors, metal protection from corrosion is mandatory requirement; among various metal protection methods application of corrosion inhibitors is most common and cost-effective strategy to prevent corrosion [3]. However, in recent years due to environment constraints over industries, usage of corrosion inhibitors mandatorily proceeds via using eco-friendly chemicals, which has low toxic effects.

Organic molecules which bearing heteroatoms viz., S-, N-, O- or π-bonds in their molecular skeleton, are reported to be an effective corrosion inhibitor [4-7]. Further, organic molecules bearing both N and S in their structure have shown better inhibition efficiency than those molecules holding only one heteroatom. In continuation of finding out organic molecules with multiple hetero atoms with less toxic effect to environment, a series of azo-coumarin dyes were synthesized and screened their inhibition potential on MS corrosion in 1.0 M HCl. The corrosion evaluation was made by employing different standard techniques viz., electrochemical impedance spectroscopy (EIS), potentiodynamic polarization and surface morphological studies using scanning electron microscopy (SEM) assessment.

2. EXPERIMENTAL

2.1. Synthesis of azo-coumarin dyes

Compounds 1-3 were dissolved in 3 mL of 11 M hydrochloric acid and subsequently cooled in the temperature range of 0-5 °C in an ice-bath. Further, sodium nitrite solution was added to the solution drop wise with vigorous stirring about 1 h, while cooling at 0-5 °C until the end of diazotization reaction. Urea (solid) was subsequently added to eliminate the excess of nitrous acid. The clear solution (4-6) was then dropwise added over cooled (range of 0-5 °C) and stirred solution of 7 in sodium acetate. The coupling mixture's pH, in each case was maintained at 8–9 by adding sodium carbonate. The reaction mixture stirred continuously at temperature 0-5 °C and the precipitated product separated upon dilution with cold water was filtered, several times washed with water, dried, and then further recrystallized by employing proper solvent to give compounds 8-10, respectively (Scheme 1) [8].

(*E*)-4-hydroxy-3-(phenyldiazenyl)-2H-chromen-2-one (8). Aniline (1) (0.30 mL, 2.5 mmol) was converted to diazonium salts (4) and treated with 4-hydroxycoumarin (7) (0.5 g, 2.1 mmol) according to the general procedure. Recrystallization of the crude product from cold ethanol afforded a yellow solid **8**. Yield 0.48 g (86%). Mp 181 – 183 °C (lit., 183 – 184 °C [8]); IR KBr (v_{max}/cm^{-1}): 3000 (Ar-H), 1615 (C=C of pyrone), 1555 (N=N), 1720 (C=O str, α pyrone), 730 (C-H out plane, mono sub phenyl); ^{1}H NMR (CDCl$_3$, 500 MHz, δ/ppm): 7.42 -7.88 (m, 9H, Ar-H), 14.58 (s, 1H, enolic OH); ^{13}C

NMR (CDCl$_3$, 125 MHz): 128.7 (C-1), 120.8 (C-2), 151.9 (C-3), 79.9 (C-4), 156.1 (C-5), 152.5 (C-6), 116.4 (C-7), 128.3 (C-8), 125.4 (C-9), 123.3 (C-10), 117.4 (C-11), 164.8 (C-12).

(*E*)-3-((4-bromophenyl)diazenyl)-4-hydroxy-2H-chromen-2-one (9). 4-bromoaniline (2) (0.43 g, 2.5 mmol) was converted to diazonium salts (5) and treated with 4-hydroxycoumarin (7) (0.5 g, 2.1 mmol) according to the general procedure. Recrystallization of the crude product from cold ethanol afforded a yellow solid 9. Yield 0.40 g (63%). Mp 225 – 228 °C (lit., 228 – 230 °C [8]); IR KBr (v_{max}/cm^{-1}): 1620 (C=C of pyrone), 1558 (N=N), 1715 (C=O str, α pyrone), 695 (Ar C-Br str), 835 (C-H out plane *para* disub phenyl); ^{1}H NMR (CDCl$_3$, 500 MHz, δ/ppm): 7.27 - 7.84 (m, 8H, Ar-H), 14.58 (s, 1H, enolic OH); ^{13}C NMR (CDCl$_3$, 125 MHz): 131.0 (C-1), 131.6 (C-2), 123.1 (C-3), 146.9 (C-4), 79.9 (C-5), 156.1 (C-6), 152.5 (C-7), 116.4 (C-8), 128.3 (C-9), 125.4 (C-10), 123.3 (C-11), 117.4 (C-12), 164.8 (C-13).

(*E*)-3-((4-chlorophenyl)diazenyl)-4-hydroxy-2H-chromen-2-one (10). 4-chloroaniline (3) (0.34 g, 2.5 mmol) was converted to diazonium salts (6) and treated with 4-hydroxycoumarin (7) (0.5 g, 2.1 mmol) according to the general procedure. Recrystallization of the crude product from cold ethanol afforded a yellow solid 10. Yield 0.44 g (61%). Mp 225 – 228 °C (lit., 228 – 230 °C [8]); IR KBr (v_{max}/cm^{-1}): 1615 (C=C of pyrone), 1555 (N=N), 1717 (C=O str, α pyrone), 772 (Ar C-Cl str), 835 (C-H def *para* disub phenyl); ^{1}H NMR (CDCl$_3$, 500 MHz, δ/ppm): 7.27 - 7.84 (m, 8H, Ar-H), 14.58 (s, 1H, enolic OH); ^{13}C NMR (CDCl$_3$, 125 MHz): 130.2 (C-1), 128.8 (C-2), 134.3 (C-3), 146.0 (C-4), 79.9 (C-5), 156.1 (C-6), 152.5 (C-7), 116.4 (C-8), 128.3 (C-9), 125.4 (C-10), 123.3 (C-11), 117.4 (C-12), 164.8 (C-13).

2.2. Corrosion evaluation

2.2.1. Preparation of mild steel specimen

Mild steel (MS) specimens of exposed area 1 cm^2 (remaining area covered with non-conductive epoxy coating) and typical composition (wt % - C - 0.08, Si - 0.01, P – 0.02, Mn - 1.26 / Fe remaining) was employed as working electrode for electrochemical analysis. The exposed MS area was wet-polished using abrasive paper with 400, 600, 800 and 1000 grades. Further, MS was immersed in distilled water and then acetone before and after electrochemical experiment.

2.2.2. Test medium

Hydrochloric acid of 1.0 M strength was prepared using 37 % AR grade hydrochloric acid by diluting it with an appropriate amount of double distilled water. The inhibitor of different concentrations (1 x 10^{-4} M to 1 x 10^{-3} M) was added into test solution to screen the concentration effect on corrosion inhibition.

2.2.3. Potentiodynamic polarization analysis

Potentiodynamic polarization studies were carried out by using a three-electrode (jacketed) cell assembly. MS with exposure area (1 cm^2) was used as a working electrode (WE), saturated calomel electrode (SCE) employed as a reference electrode (RE) and platinum wire applied as a counter electrode (CE). The measurements were carried out using Gamry Instrument Reference 600 at room temperature. The open circuit potential, E_{ocp} was monitored and noted for 1800 s in-order-to reach steady-state potential. Further, polarization studies were carried over the test medium (1.0 M HCl) in presence and absence of corrosion inhibitor at potential range of ± 250 mV with respect to E_{ocp} at scan rate 0.5 mVs^{-1}. The inhibition efficiency values (IE %) were calculated by using equation 1 [9].

$$IE \% = \frac{I_{corr} - I_{corr\,(i)}}{I_{corr}} \times 100 \% \tag{1}$$

Where, I_{corr} and $I_{corr(i)}$ are corrosion current density values in absence and presence of corrosion inhibitor respectively. Corrosion rate was calculated by using the following equation 2:

$$CR\,(mpy) = \frac{0.13 \times i_{corr} \times M_{ew}}{\rho} \tag{2}$$

2.2.4. Electrochemical impedance spectroscopy (EIS) analysis

The EIS study was carried out in Gamry potentiostat (model 600). After OCP stabilization for 1800 s, EIS was performed at frequency range of 10 kHz - 0.01 kHz at scan rate of 0.5 mVs^{-1} and signal amplitude perturbation of 5 mV. The resultant Nyquist plots were tested to fit with equivalent circuit models provided in Echem Analyst software. The inhibition percentage (IE %) was evaluated by using following equation 3 [9].

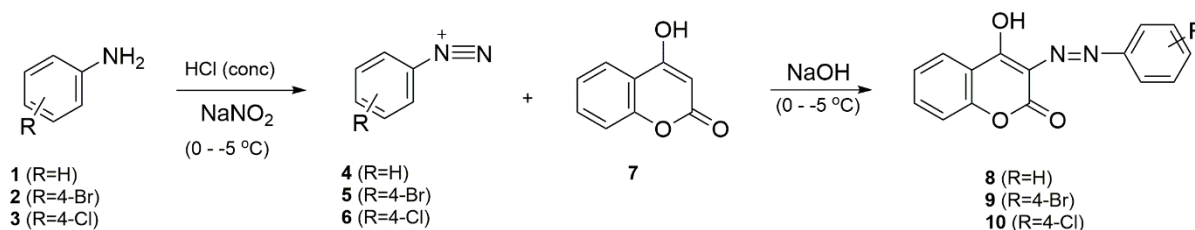$$IE \% = \frac{R_{ct(i)} - R_{ct}}{R_{ct(i)}} \times 100 \% \tag{3}$$

Where R_{ct} and $R_{ct(i)}$ are charge transfer resistance values in absence and presence of inhibitor, respectively.

2.2.5. Surface morphology analysis

MS surface was screened in scanning electron microscope combined with energy dispersive X-ray spectroscopy (SEM/EDX) in instrument model Quanta FE I 650. For this analysis, the test specimen exposed to electrolyte that contains the inhibitor which exhibit the highest inhibition efficiency from electrochemical studies. This analysis and then compared to the test specimen exposed to blank solution at the same magnification.

3. RESULT AND DISCUSSION

3.1. Synthesize of azo-coumarin dyes

Scheme 1. Synthesis of azo-coumarin dyes **8**-**10**

The azo-coumarin dyes series (8-10) was synthesized successfully by coupling reaction of diazonium salts (4-6) of four different substituted aniline derivatives (1-3) with 4-hydroxycoumarin (7) in the presence of basic condition shown in Scheme 1 [10]. Diazotisation was carried out along with nitosyl hydrochloric acid and excess of nitrous acid is destroyed by the addition of urea [11]. All compounds were determined and elucidated by using spectroscopic methods and consistent with the reported value from literatures [8]. A series of synthesized azo-coumarin dyes were summarized in Fig. 1.
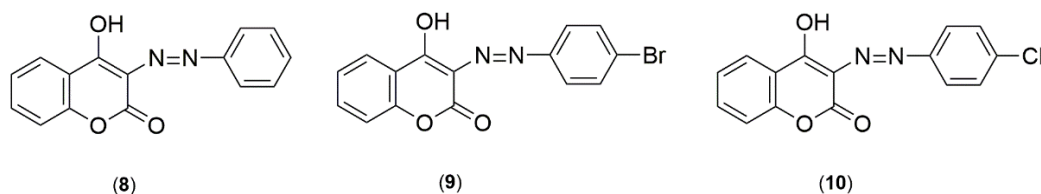

Figure 1. Azo-coumarin dyes 8-10

3.2. Electrochemical studies

3.2.1. Polarization analysis

Potentiodynamic polarization screening was carried out to investigate the effect of inhibitors (azo-coumarin dyes 8-10) on the kinetic of cathodic and anodic reaction. The polarization results depicted in Fig. 2 and the corrosion parameters viz., corrosion current density (i_{corr}), corrosion potential (E_{corr}), cathodic and anodic current density (β_a and β_c) are summarized in Table 1.
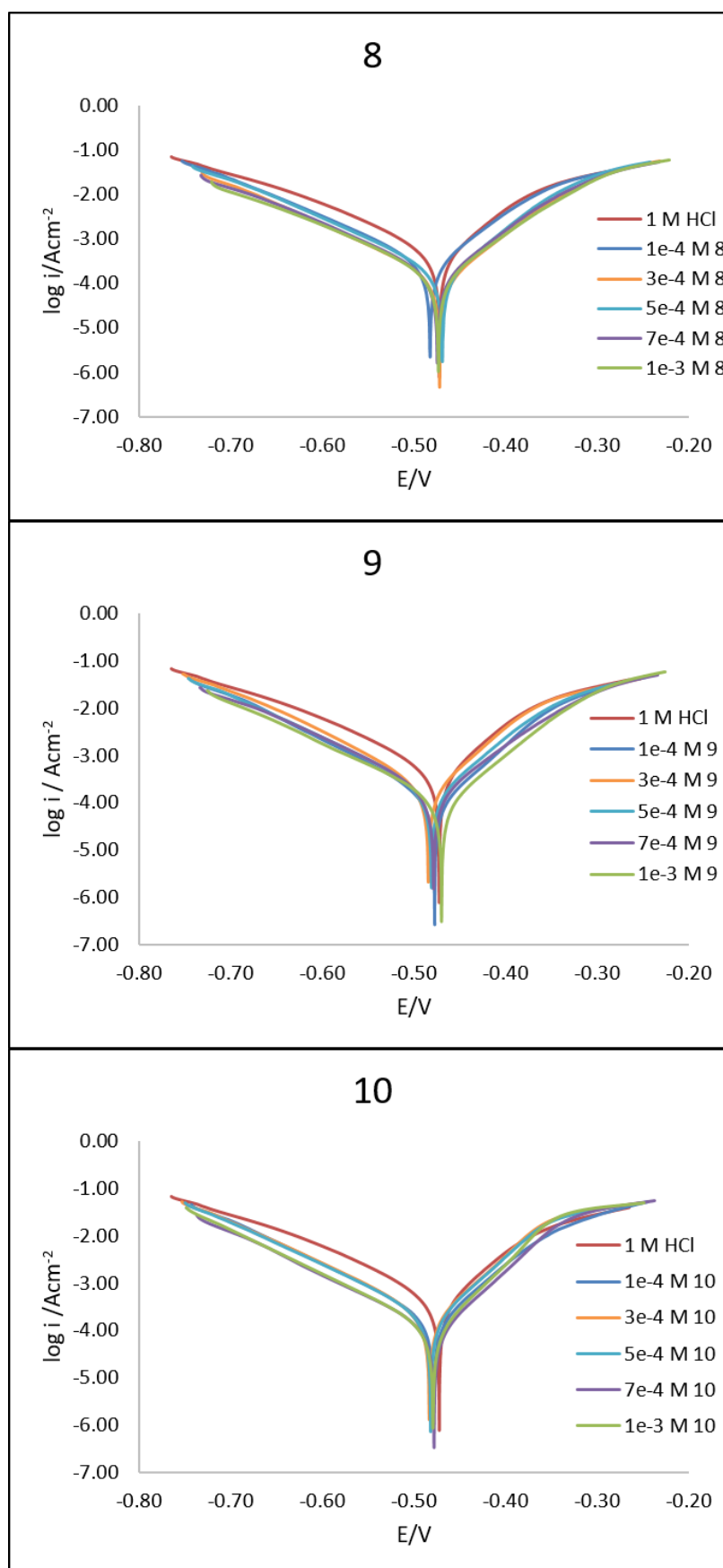
Figure 2. Potentiodynamic polarization curves (vs. SCE) for the corrosion of mild steel with different concentrations of corrosion inhibitors **8**-**10**, and without the addition of inhibitor in 1.0 M HCl
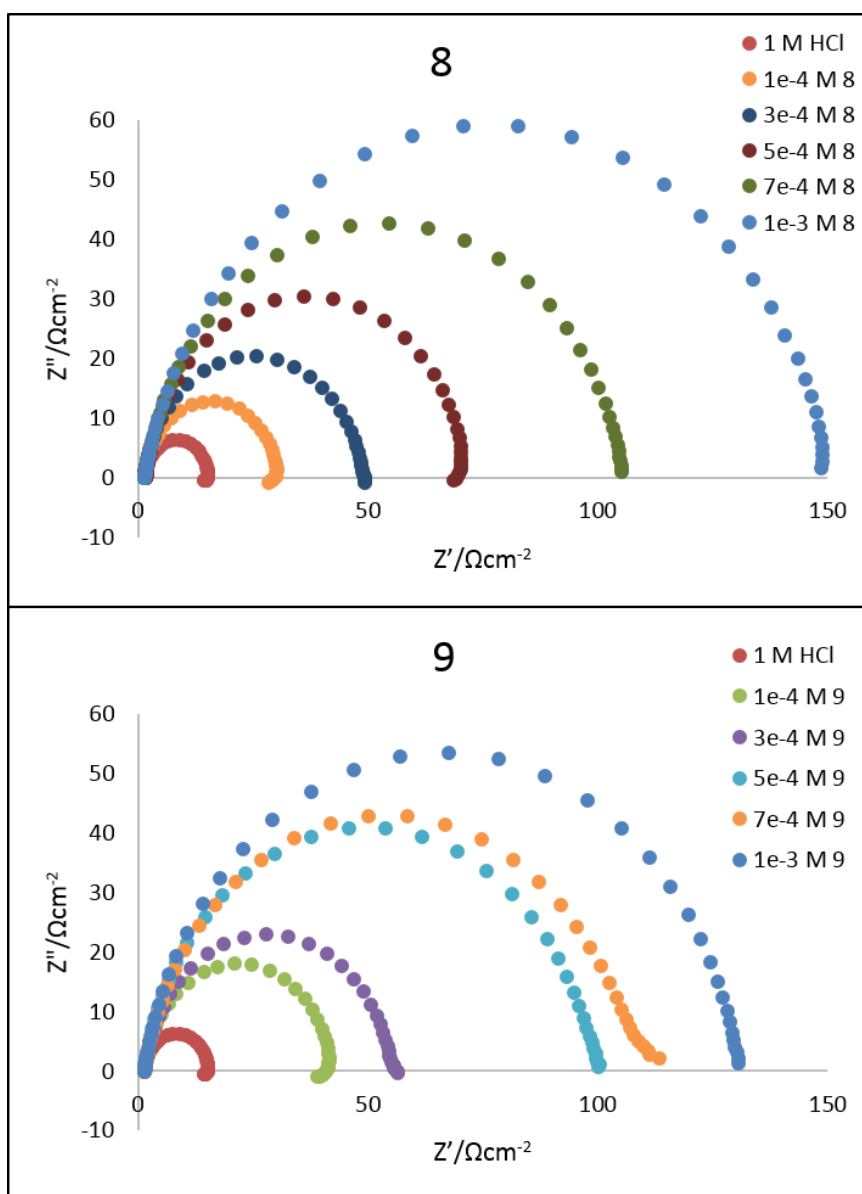
Table 1. Electrochemical polarization parameters for corrosion of mild steel in the absence and presence of different concentration of inhibitors 8-10 in 1.0 M HCl solution.

Inhibitor	Concentration (M)	E_{corr} (mV)	i_{corr} (A/cm^2)	β_a (mV/decade)	$-\beta_c$ (V/decade)	Corrosion rate (mpy)	% *IE*
Blank (HCl)	1.0	-473	5.870×10^{-4}	74	108	273	-
8	1.0×10^{-4}	-483	2.424×10^{-4}	70	101	113	59
	3.0×10^{-4}	-472	1.814×10^{-4}	88	109	84	69
	5.0×10^{-4}	-469	1.460×10^{-4}	70	109	68	75
	7.0×10^{-4}	-474	1.110×10^{-4}	91	122	52	81
	1.0×10^{-3}	-473	6.309×10^{-5}	94	127	29	89
9	1.0×10^{-4}	-479	2.670×10^{-4}	126	184	124	54
	3.0×10^{-4}	-484	2.030×10^{-4}	71	97	94	65
	5.0×10^{-4}	-482	1.760×10^{-4}	69	106	82	70
	7.0×10^{-4}	-478	1.150×10^{-4}	87	141	53	80
	1.0×10^{-3}	-479	1.000×10^{-4}	63	104	76	83
10	1.0×10^{-4}	-477	2.530×10^{-4}	114	191	118	57
	3.0×10^{-4}	-484	2.220×10^{-4}	75	98	103	62
	5.0×10^{-4}	-481	1.740×10^{-4}	76	95	81	70
	7.0×10^{-4}	-474	1.259×10^{-4}	88	103	59	78
	1.0×10^{-3}	-470	7.943×10^{-5}	109	141	37	86

Potentiodynamic polarization curves of azo-coumarin inhibitors, showed decrease of corrosion current density values as compared with blank 1.0 M HCl test solution which evident the corrosion rate reduced. The reduction current density probably due to the presence of hetero (azo) group in azo-coumarin derivatives which may merely blocks the reactive sites over MS surface [12]. The percentage inhibition efficiency maximum was resulted for concentration of 1×10^{-3} M (IE compound 9: 82.96% < IE compound 10: 86.46% < IE compound 8: 89.25%). Subsequently, the corrosion rate was significantly reduced with the addition of inhibitor 8-10, and corrosion rate (*CR*) minimum was found at highest concentration vof inhibitors (compound 8: 29.36 mpy < compound 10: 36.97 mpy < compound 9: 46.55 mpy).

Further, the shift of corrosion potential (E_{corr}) values for inhibitors with respect to blank solution provides information on the type of corrosion inhibition. Corrosion potential values for azo-coumarin inhibitors 8-10 not showed significant shift in either anodic or cathodic side which suggest the mixed type corrosion inhibition. This was well supported by the cathodic (β_c) and anodic (β_a) slope values, which showed only negligible variation for inhibitor (compounds 8-10) when compared with blank values. Earlier, Haiduc et al., reported that when E_{corr} shift in anodic / cathodic side is greater than 85 mV, the inhibitor may considered to be act as anodic / cathodic type of inhibitors [11]. While the E_{corr} shift is within 85 mV range, the inhibitor considered to be act as a mixed-type inhibitor. In our case, the coumarin inhibitors found to shift E_{corr} values within 10 mV range and hence considered as mixed type of corrosion inhibitors.

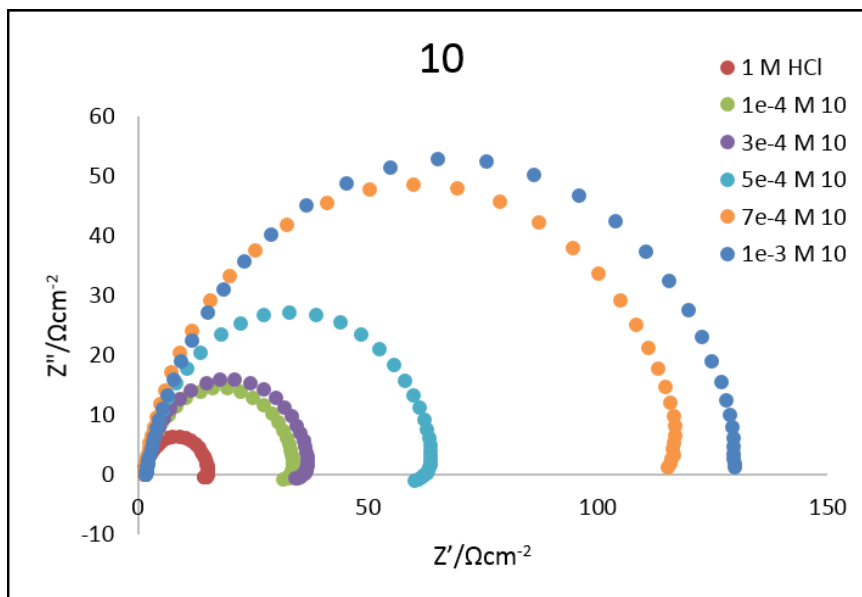### 3.2.2. Electrochemical impedance spectroscopy (EIS) analysis

Figure 3. Nyquist plots (vs. SCE) of mild steel plates immersed in various concentration of inhibitors 8-10 in 1.0 M HCl

Table 2. Electrochemical impedance parameter for mild steel in the absence and presence of different concentration of inhibitors 8-10 in 1.0 M HCl solution.

Inhibitor	Concentration (M)	R_s (Ωcm^2)	R_{ct} (Ωcm^2)	CPE ($mFcm^{-2}$)	n	IE%
Blank (HCl)	1.0	1.336	13.80	0.3005	0.9361	-
8	1.0×10^{-4}	1.339	28.71	0.2917	0.9215	52
	3.0×10^{-4}	1.349	47.64	0.2518	0.9168	71
	5.0×10^{-4}	1.780	69.09	0.2496	0.9099	80
	7.0×10^{-4}	1.444	104.10	0.2467	0.8779	87
	1.0×10^{-3}	1.452	148.70	0.2153	0.8596	90
9	1.0×10^{-4}	1.365	40.10	0.2448	0.9214	65
	3.0×10^{-4}	1.385	54.10	0.2392	0.9168	74
	5.0×10^{-4}	1.436	97.79	0.2366	0.9016	86
	7.0×10^{-4}	1.522	106.90	0.2316	0.8941	87
	1.0×10^{-3}	1.471	129.20	0.2153	0.8831	89
10	1.0×10^{-4}	1.538	32.14	0.2797	0.9361	57
	3.0×10^{-4}	1.532	35.24	0.2532	0.9256	61
	5.0×10^{-4}	1.460	62.51	0.2312	0.9007	78
	7.0×10^{-4}	1.420	116.60	0.2161	0.8872	88
	1.0×10^{-3}	1.739	130.80	0.2035	0.8538	89

EIS measurement was carried out for MS corrosion in 1.0 M HCl in the presence and absence of coumarin inhibitors and the results are depicted as Nyquist plot (Fig. 3). EIS parameters viz., charge transfer resistance (R_{ct}) and constant phase element (*CPE*) derived are listed in Table 2. Based on the

Nyquist plots, it is evident that when the concentration of azo-coumarin dyes 8-10 increases, the diameters of the resistance charge transfer (R_{ct}) increases. Electrochemical theory stated that, charge transfer resistance (R_{ct}) and corrosion current density (I_{corr}) are inversely proportional to each other [13]. The charge transfer resistance values were found increasing along with increasing coumarin's concentration, which may be result in many inhibitor molecules adsorbed over MS surface at higher concentration of inhibitors [14]. Thus, our experiment results in Table 2 suggested that when the inhibitor concentration increased inhibition efficiency increased, conversely the corrosion rate found decreased.

From the Nyquist plot (Fig. 3), the optimum concentration of all the azo-coumarin dyes 8-10 tested was found as 1 x 10^{-3} M, which given the highest charge transfer resistance, R_{ct}. The optimum concentrations showed following maximum corrosion inhibition efficiency (compound 9: 82.96% < compound 10: 86.46% < compound 8: 89.25%).
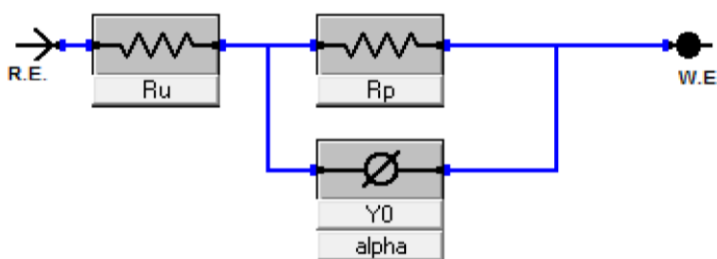

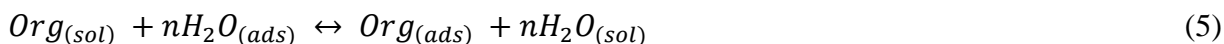**Figure 4.** Equivalent circuit used for EIS data fitting

The circuit for constant phase element (CPE) was employed as an equivalent circuit (Fig. 4) to be fitted and analysed with the experimental data in order to gain more closely matching fit. In general, shape of CPE is referred to the roughness / inhomogeneity on working electrode or to the dielectric constant [12]. For coumarin derivatives, CPE values were found decreased when their concentrations increased, which suggesting that local dielectric constant reduced and/or thickness of the electrical double layer increased [9]. The CPE's impedance can be expressed by using equation 4.

$$Z_{CPE} = {1}/{Y_o (j\omega)^n} \tag{4}$$

Where, Y_o is CPE's magnitude CPE, ω is the angular frequency ($\omega = 2\pi f$, where f is the AC frequency), j is the imaginary unit, and n is the phase shift (CPE exponent).

3.2.3. Adsorption isotherm

The adsorption phenomena of corrosion inhibitors depend on the molecular structures of the inhibitors, nature / charge on the MS surface and electron charge distribution on inhibitor molecule [15]. Usually, corrosion inhibitor adsorbed over metal surface through removal of adsorbed water molecule and being displaced by dissolved organic corrosion inhibitors molecules from the aqueous medium. The possible mechanism involved is as shown in following reaction equation 5.

$$Org_{(sol)} + nH_2O_{(ads)} \leftrightarrow Org_{(ads)} + nH_2O_{(sol)} \tag{5}$$

where $Org_{(aq)}$ and $Org_{(ads)}$ are the organic corrosion inhibitor molecules in aqueous solution, which are adsorbed over metal surface; while, $H_2O_{(ads)}$ is water molecules which are being replaced with unit of inhibitor [16].
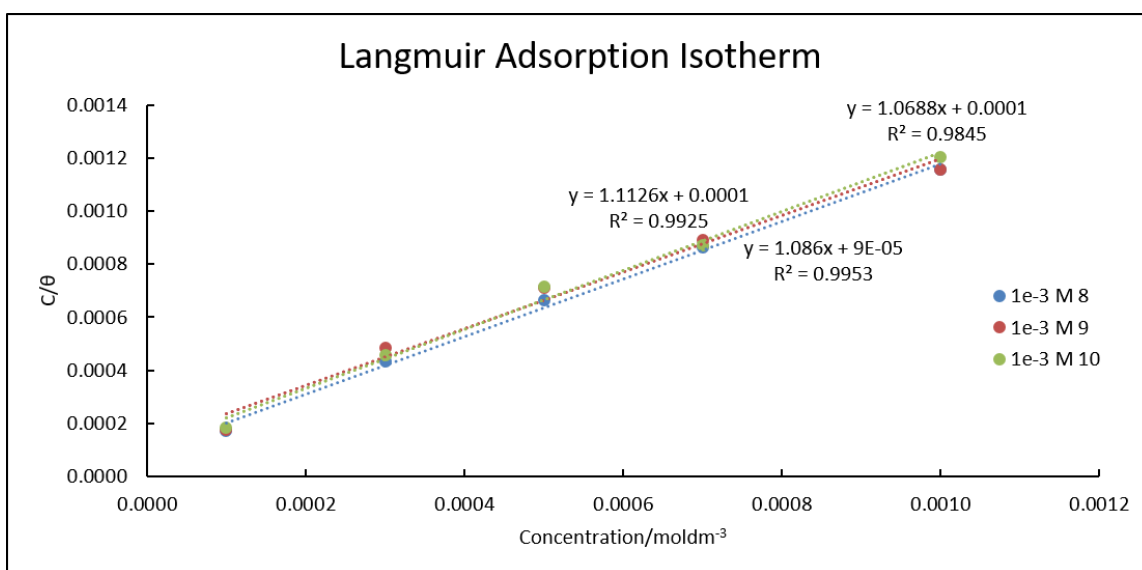

Figure 5. Langmuir adsorption isotherm plots in varying concentration of inhibitors 8-10 in 1.0 M HCl solution.

The surface coverage, θ was calculated from IE % / 100 and the data obtained were fitted with different adsorption isotherms viz., Frumkin, Temkin and Langmuir. The data were found fit well with Langmuir adsorption isotherm as shown in Fig. 5. A good linearity of the Langmuir isotherm ($R_2(8)$: 0.9845, $R_2(9)$: 0.9925, $R_2(10)$: 0.9953) assumed that the inhibitor formed a monolayer protection over the interface of MS specimen [17]. The Langmuir isotherm is represented in equation 6 below:

$$C/_\theta = 1/_{K_{ads}} + C \tag{6}$$

Where, K_{ads} is the equilibrium constant of adsorption – desorption process, θ is the surface coverage (IE % / 100), and C is the concentration of corrosion inhibitor in mol dm^{-3}. From K_{ads} values, $\Delta G°_{ads}$ (Gibbs free energy of adsorption) was calculated by using equation 7.

$$\Delta G^{\circ}_{(ads)} = -RT \ln (K_{ads} \times A) \tag{7}$$

Where, A denoted water's molar concentration (55.5 moldm^{-3}), R denoted the universal gas constant (8.314 J K^{-1} mol^{-1}) and T denoted the temperature of the system in Kelvin.

The obtained negative ΔG°_{ads} values implied that the adsorption of azo-coumarin dyes over MS surface was spontaneous process [18]. Further, ΔG°_{ads} values also provide significant details on corrosion inhibition mechanism. Generally, when the ΔG°_{ads} value obtained is within -20 kJ mol^{-1} indicates that the adsorption process follow the physisorption mechanism. Meanwhile, if the ΔG°_{ads} value obtained is above -40 kJmol^{-1} indicates that the adsorption process will follow chemical adsorption mechanism. Thus, it was predicted that azo-coumarin dyes 8-10 inhibitor will be physically or semi-chemically adsorbed over MS surface, since the resultant ΔG°_{ads} value for compounds 8-10 are -33 kJ mol^{-1}, -27 kJ mol^{-1} and -27 kJ mol^{-1}, respectively. These values suggest that the adsorption on mild steel surface in 1.0 M HCl was physisorption [19].

3.3. Surface analysis

3.3.1 Corrosion inhibition mechanism

In the test solution (1.0 M HCl), an assumption can be made that the chloride anions will adsorb over the positively charge MS surface as in equation 8:

$$Fe + Cl^{-} \leftrightarrow (FeCl^{-})_{ads} \tag{8}$$

It was proposed that the corrosion inhibitor molecules get protonated in acidic media, which are further adsorbed over negatively charged MS surface through electrostatic force of interactions. Corrosion inhibition mechanism may either proceed via physisorption (electrostatic force of interaction) or chemisorption of azo-coumarin dyes may happened via electron donor acceptor interactions between organic inhibitor's hetero atoms / π electron clouds on phenyl ring and iron's vacant 'd' orbital [20]. The adsorption isotherms analysis and ΔG°_{ads} values clearly evident that all the azo-coumarin dyes 8-10 was predominantly physisorption, which means that only electrostatic force of interaction involved between azo-coumarin dyes and MS surface (Fig. 6). El-Haddad and Fouda [21] proposed a comparable mechanism to that presented in this study.
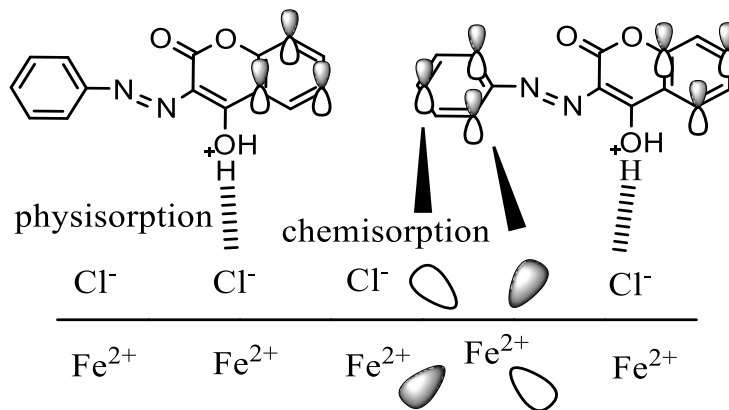
Figure 6. Corrosion inhibition mechanism of azo-coumarin dyes over mild steel in 1.0 M HCl solution

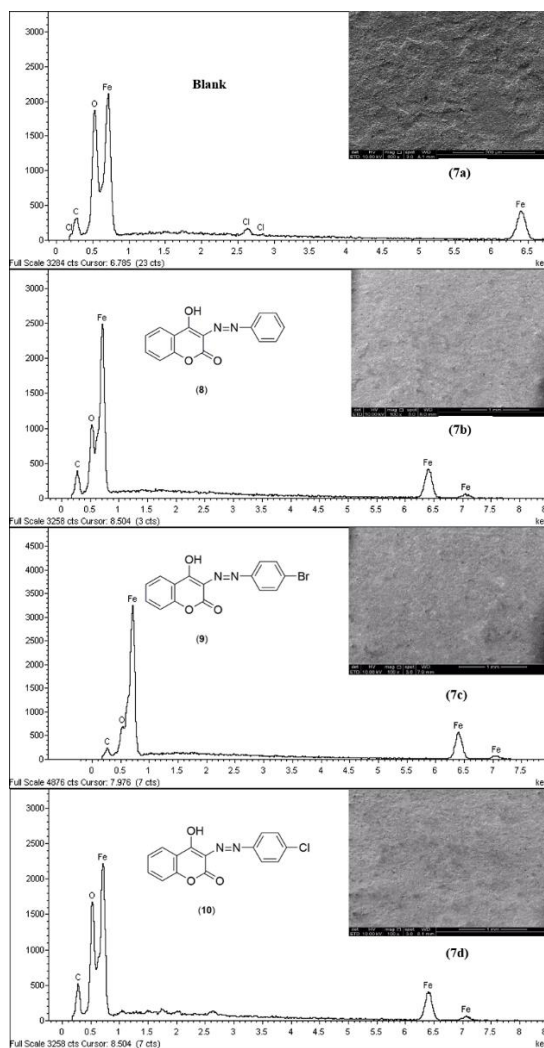### 3.3.2. *SEM/EDX analysis*

Figure 7. SEM micrographs of mild steel after immersion in 1.0 M HCl solution for 24 hours with the absence of inhibitors (7a), and in the presence of inhibitors: 1.0 mM of 8 (7b), 9 (7c) and 10 (7d), respectively.

Corrosion inhibition process on MS surface was further screened via SEM and EDX microscope. The microscopy images obtained were shown in Fig. 7a (blank solution) and Fig. 7b-d (immersed with azo-coumarin inhibitors). From the results, it is evident that the MS immersed in 1.0 M HCl solution with azo-coumarin inhibitors has smooth surface (in particular for compound 8) as compared with MS in blank 1.0 M HCl medium. This investigation unfolded that the corrosion rate decreased significantly with the inclusion of inhibitor on mild steel [22]. Further, the atomic content percentage of MS specimen was obtained through EDX screening and are listed in Table 3; which revealed that the corrosion products (ferric hydroxide / oxyhydroxides) formation due to severe oxidation of FeCl [23]. However, the EDX spectra of coumarin inhibitors showed the reduced intensity of oxygen atom, which confirming that the azo-coumarin dyes act as efficient inhibitor for MS corrosion 1.0 M HCl medium. Based on findings from SEM and EDX, it showed that azo-coumarin inhibitors had a capability to form a stable inhibitive film on mild steel surface to offer resistance against corrosion [24].

Table 3. Percentage of atomic elements in mild steel specimens obtained from EDX spectra

MS specimen	Element (% atomic)			
	Fe	**O**	**C**	**Cl**
Blank	68.81	25.77	4.46	0.96
1×10^{-3} M of **8**	79.93	15.31	4.76	-
1×10^{-3} M of **9**	76.83	15.62	7.55	-
1×10^{-3} M of **10**	78.62	13.01	8.28	-

4. CONCLUSION

Three azo-coumarin dyes were prepared by the coupling reaction between diazonium salt of aniline derivatives and 4-hydroxycoumarin in basic conditions. The azo-coumarin dyes were obtained by relatively simple synthesis methods with high and good reaction yields (61-86 %). The structures of azo-coumarin dyes were successfully characterized via Infrared Spectroscopy (IR) and Nuclear Magnetic Resonance (^{1}H NMR and ^{13}C NMR) spectroscopy. The azo-coumarin dyes have been further screened for corrosion inhibition potential for MS corrosion in 1.0 M HCl medium, using electrochemical impedance and polarization techniques. The results confirmed that all the azo-coumarins 8 - 10 were acted as efficient corrosion inhibitors and shown average *IE* > 80%. The coumarin inhibitors inhibited corrosion via adsorption process, which was found to follow Langmuir adsorption isotherm. The adsorption was spontaneous and the inhibition of corrosion by azo-coumarin inhibitors was due to formation of physical adsorption on the mild steel surface. SEM – EDX analysis well supported for the electrochemical analysis and provide additional evidence for the adsorption of inhibitors over MS surface.

References

1. I. Ahamad and M. A. Quraishi, *Corros. Sci.*, 51 (2009) 2006.
2. C. Verma, E. E. Ebenso, and M. A. Quraishi, *J. Mol. Liq*., 233 (2017) 403.
3. X. Li, S. Deng, H. Fu, and T. Li, *Electrochim. Acta*, 54 (2009) 4089.
4. E. Adbelghani, M. A. Amin, and H. H. Hassan, *Electrochim. Acta,* 52 (2007) 6359.
5. E. Altunbaz, G. Kardas, and R. Solmaz, *Prot. Met. Phys. Met.*, 47 (2011) 262.
6. M. A. Amin, R. S. Boyoumi, S. S. El-Rahim, and E. E. F. El-Sherbini, *Electrochim. Acta*, 52 (2007) 3588.
7. Q. He, B. Hou, W. Li, and C. Pei, *Electrochim. Acta*, 52 (2007) 6386.
8. A. Ghanadzadeh, E. Moradi, and M. R. Yazdanbakhsh, *J. Mol. Liq*., 136 (2007) 165.
9. T. S. Hamidon, and M. H. Hussin, *Prog. Org. Coat*., 140 (2020) 105478.
10. B. T. Abhinav, and S. Nagaiyan, *J. Fluoresc.,* 26 (2016) 1279.
11. I. Haiduc, I. Sebe, and E. G. H. Shahinian, *U. P. B. Sci. Bull. Series B Chem. Mater. Sci.*, 73 (2011) 153.
12. H. Hamani, T. Douadi, M. Al-Noaimi, S. Issaadi, D. Daoud, and S. Chafaa, *Corros. Sci*., 88 (2014) 234.
13. M. Behpour, B. Ebrahimi, S. M. Ghoreishi, and M. S. Niasari, *Mater. Chem. Phys.*, 107 (2008) 153.
14. B. Maiti, M. A. Quraishi, and D. K. Yadav, *Corros. Sci.,* 52 (2010) 3586.
15. M. H. Hussin, and M. J. Kassim, *Mater. Chem. Phy.*, 125 (2011) 461.
16. M. H. Hussin, N. Brosse, M. N. M. Ibrahim, and A. A. Rahim, *Measurement*, 78 (2016) 90.
17. M. H. Hussin, N. Brosse, M. N. M. Ibrahim, and A. A. Rahim, *Mater. Chem. Phys.,* 163 (2015) 201.
18. S. Adnan, A. A. Hussain, and A. Nabi, *Journal of Basrah Researches (Sciences)*, 38 (2012) 125.
19. M. Mohammad and R. Marziya, *Carbohydrat. Polym*., 160 (2017) 172.
20. P. Muthukrishnan, B. Jeyaprabha, and P. Prakash*, Arabian J. Chem.,* 10 (2008) 2343.
21. M. N. El-Haddad and A. S. Fouda, *Chem. Eng. Comm.,* 200 (2013) 1366.
22. N. A. Rozuli, T. S. Hamidon, and M. H. Hussin, *Mater. Res. Express*, 6 (2019) 106524.
23. F. Bentiss, M. Outirite, M. Traisnel, H. Vezin, M. Lagrenée, B. Hammouti, S. S. Al-Deyab, and C. Jama, *Int. J. Electrochem. Sci.*, 7 (2012) 1699.
24. R. A. Prabhu, T. V. Venkatesha, and A. V. Shanbhag, *J. Iran. Chem. Soc*., 660 (2009) 353.